Environmental Pollution 224 (2017) 421–429

Contents lists available at ScienceDirect

Environmental Pollution

journal homepage: www.elsevier.com/locate/envpol

Stack and fugitive emissions of major air pollutants from typical brick kilns in China☆

Yuanchen Chen [a, b], Wei Du [a], Shaojie Zhuo [a], Weijian Liu [a], Yuanlong Liu [c], Guofeng Shen [d], Shuiping Wu [c], Jianjun Li [e], Bianhong Zhou [e], Gehui Wang [e], Eddy Y. Zeng [f], Hefa Cheng [a], Wenxin Liu [a], Shu Tao [a, *]

[a] Laboratory for Earth Surface Processes, College of Urban and Environmental Sciences, Peking University, Beijing 100871, China
[b] College of Environment, Zhejiang University of Technology, Hangzhou 310014, China
[c] College of the Environment and Ecology, Xiamen University, Xiamen 361102, China
[d] ORISE Postdoctoral Fellow at National Risk Management and Research Laboratory (NRMRL), U.S. Environmental Protection Agency, Durham, NC 27713, USA
[e] Institute of Earth Environment, CAS, Xi'an 710075, China
[f] School of Environment, Guangzhou Key Laboratory of Environmental Exposure and Health and Guangdong Key Laboratory of Environmental Pollution and Health, Jinan University, Guangzhou 510632, China

ARTICLE INFO

Article history:
Received 19 December 2016
Accepted 11 February 2017
Available online 22 February 2017

Keywords:
Major pollutants
Brick kilns
Fugitive emission
Stack emission
New calculating method

ABSTRACT

Little information exists on emission factors (EFs, quantities of pollutants emitted per unit of fuel consumed) for brick kilns in China, although brick kilns are important emission sources of many air pollutants, and 45% of the world's bricks are produced in China. In this study, EFs of carbon dioxide (CO_2), carbon monoxide (CO), sulfur dioxide (SO_2), nitrogen oxides (NOx), particulate matters (PMs), black carbon (BC), organic carbon (OC), and polycyclic aromatic hydrocarbons (PAHs) for brick kilns were derived based on field measurements of a total of 18 brick kilns of major types in China. This was the first study to quantify EFs of both stack and fugitive sources based on a modified carbon balance method that was developed for this study. The EFs of most pollutants, especially the incomplete combustion products in fugitive emissions, were much higher than those for stack emissions, indicating a substantial underestimation of total emissions when leakage is not taken into consideration. This novel method can be applied to quantify emissions from other similar sources with both stack and fugitive emissions.

1. Introduction

The massive health impact associated with air pollution is definitely one of the major environmental concerns in China (Matus et al., 2011; Kan et al., 2012). The severe air pollution is primarily caused by emissions of a large number of pollutants from various sources (Seinfeld and Pandis, 2016; Smith, 1987). The characterization and quantification of the emissions are critical for quantitatively assessing the impacts. Among a variety of emission sources, brick kilns are important in developing countries where fired bricks are extensively manufactured. There are approximately 80,000 brick kilns in China (Centre for Science and Environment, 2015), of which 90% are the traditional annular type (General Administration of Quality Supervision, 2013). It was estimated that China produced 340 billion bricks in 2012 (Baum, 2015; National Bureau of Statistics of the People's Republic of China, 2013), contributing 44% of the global total production (Centre for Science and Environment, 2015). The emissions of air pollutants from brick production depend very much on the type of kiln and fuel used. Low-quality coal is widely used in fired brick production (Zhang, 1997), resulting in high emissions of air pollutants (Huang et al., 2014; Wang et al., 2014; Shen et al., 2013a).

Although brick kilns in China are important emission sources, emission factors (EFs, quantities of pollutants emitted per unit of fuel consumed) are not available, except a few values for total suspended particles (TSP) and nitrogen oxides (NOx) (Zhao et al., 2013; National Bureau of Statistics of the People's Republic of China, 2009). Therefore, the total emissions of various pollutants from this sector can only be estimated based on the EFs measured

☆ This paper has been recommended for acceptance by David Carpenter.
* Corresponding author.
E-mail address: taos@pku.edu.cn (S. Tao).

http://dx.doi.org/10.1016/j.envpol.2017.02.022
0269-7491/

in other countries (Baum, 2015; Maithel et al., 2012; Guttikunda, 2015). Since most brick kilns in China are different from those operated in other countries, this estimation can lead to considerable bias in emission inventories (Huang et al., 2014; Wang et al., 2014; Shen et al., 2013a).

Like many other similar processes, emissions of air pollutants from brick kilns occur not only through chimneys but also from leakage (Skinder et al., 2013). For example, the annular brick kilns usually have large furnaces with large roof areas but only a single chimney; therefore, leakage from the furnace is enormous. Unfortunately, all EF measurements for brick kilns were conducted by collecting only stack gas samples at chimneys, thereby omitting fugitive emissions (Maithel et al., 2012; Reddy and Venkataraman, 2002). The reason for this practice is the technical difficulty of sampling fugitive emission quantitatively. It is likely that the true emission rates of air pollutants from brick kilns are much higher than those reported.

The carbon balance method is often used for EF determination based on the measurements at chimneys without weighing the fuels. The basic assumption of the method is that the quantity of the consumed fuel carbon equals the emitted fuel carbon (Shen et al., 2010). The concept was utilized in this study. If only the quantity of fuel carbon is known, the carbon balance method can be modified to quantify fugitive emissions by assuming that the quantity of fuel carbon equals that emitted via both chimney and fugitive pathways (see Methodology section). To the best of our knowledge, this is the very first time that EFs for brick kilns were quantified for both point and fugitive sources.

The objective of this study was to measure emissions of a series of air pollutants, including carbon monoxide (CO), carbon dioxide (CO_2), sulfur dioxide (SO_2), NOx, TSP, PM_{10} (PM with mean aerodynamic size less than 10 μm), $PM_{2.5}$ (less than 2.5 μm), black carbon (BC), organic carbon (OC), pPAHs (parent polycyclic aromatic hydrocarbons (PAHs)), nPAHs (nitro-PAHs), and oPAHs (oxy-PAHs) from two typical types of annular brick kilns in China. The EFs of these pollutants were quantified for both stack and fugitive emissions. The differences between the two pathways and the two kiln types are addressed. In addition, the relationship among the pollutants is discussed.

2. Methodology

2.1. The brick kilns and study sites

Two of the most popular types of annular brick kilns (Hoffman kilns) (Fig. S1) with two air ducts were studied. A total of 18 kilns in Xiamen (K-1) in Southern China (July 2013) and 10 kilns in the Xi'an-Baoji-Weinan area (K-2) in Northern China (Dec. 2014) were measured for emissions. The detailed descriptions are provided in Table S1. The major differences are that 1) the K-2 kilns have permanent brick roofs with numerous fuel feeding holes, while the roofs of K-1 kilns are loosely covered with coal slag and brickbats with countless cracks in between (Fig. S2); 2) the K-2 kilns (approximately 40 m in length) are smaller than the K-1 kilns (approximately 60 m in length); and 3) the chimney heights are 20–30 m and 1–1.5 m (Fig. S3), and the exhaust fans are 11 and 7 kW for K-1 and K-2 kilns, respectively. For both types of kilns, crushed coal is mixed with unfired bricks and is frequently fed into the furnace through feeding holes or cracks during the operation. The average fuel consumption of K-2 (0.12 kg/brick) is slightly higher than that of K-1 (0.10 kg/brick), and the coal properties are similar (Table S2).

2.2. On-site measurements

Measurements were conducted for CO, CO_2, NO, NO_2, and SO_2 at the chimneys (stack gas) for all kilns and on the furnace roof (fugitive gas) of eight K-1 and five K-2 randomly selected kilns. To account for variation in fugitive emissions, the fugitive emission measurements were conducted a minimum of 15 randomly selected locations for K-1 or five fuel feeding holes for K-2. The measurements at the stacks and on the furnace roofs were conducted simultaneously for each kiln. For each kiln, duplicate measurements were conducted with each measurement lasting for at least 40 min at two-second intervals. CO and CO_2 were measured using a GXH-3051 CO/CO_2 analyzer (Junfang Tech. Beijing, China), and NO, NO_2, and SO_2 were determined using a JFQ-3150E N-S analyzer (Junfang Tech. Beijing, China). The instruments were calibrated in the laboratory and zero-calibrated immediately prior to each measurement on site. The combustion temperatures were measured by inserting a probe (DT-625, CEM, Shenzhen, China) into the fuel feeding holes or cracks.

2.3. Sample collection and analysis

Stack and fugitive gas samples were collected during the on-line measurements and used for analyzing the pollutants, including $PM_{2.5}$, PM_{10}, TSP, EC, OC, pPAHs, nPAHs, and oPAHs. $PM_{2.5}$ and PM_{10} samples were collected on glass fiber filters using impaction samplers (PEM, SKC, USA), while TSP, EC, OC and particulate phase PAHs samples were trapped on quartz fiber filters (QFFs) using regular samplers (Pall Co. USA). Polyurethane foam (PUF, 0.024 g/cm^3, 22 mm in diameter and 7.6 cm in length) was used to collect gaseous phase PAHs. All pumps were calibrated against a flow rate calibrator (Bios Defender 510, USA). All samples were collected and measured in duplicate.

2.4. Sample analysis and data analysis

The sample analysis was conducted following the same procedures used previously (Shen et al., 2010; Chen et al., 2016a, 2016b, 2016c; Shen et al., 2011). The detailed procedures of the sample analysis and quality control are provided in the Supporting Information (S1).

EFs were calculated using the modified carbon balance method for stack and fugitive emissions individually. The results were all converted to mass of the pollutants emitted per unit of fuel consumed (g/kg, mg/kg). The average stack flow rates were calculated based on the measured chimney diameter and the flow velocities at a number of points at the stack cross-section using an anemoscope (SFC-D-01, Yemao, China). The fugitive flow rate of a kiln was calculated using the modified carbon balance method (Supporting Information, S2), and the overall EFs were derived as sums of the EFs for the two pathways. For the statistical analysis, SPSS 13.0 (SPSS Inc. USA) was used, and a significance level of 0.05 was considered statistically significant. For the multivariate analysis, the EFs were log-transformed and normalized.

3. Results and discussions

3.1. The measured emission factors

The statistics of the measured EFs of various pollutants are summarized in Tables 1 and 2 for the stack flue gas and fugitive emissions, respectively. The EFs of most air pollutants are often reported to be log-normally distributed (Adgate et al., 2002; Peng et al., 2011). Log-normal distributions were also observed for the EFs measured in this study, and several typical examples are shown

Table 1
The EFs of various air pollutants measured for stack flue gas of the two types of brick kilns. The statistics include the arithmetic means (M) standard deviations (SD), geometric means (GM), and the 25th, 50th, and 75th percentiles (p25, p50, and p75).

Pollutants	K-1						K-2						
	M	SD	GM	p25	P50	p75	M	SD	GM	p25	p50	p75	
CO_2	g/kg	1940	260	1930	1860	1980	2090	1920	240	1910	1760	1860	2120
CO	g/kg	267	161	222	142	245	325	395	160	358	282	442	488
EC	g/kg	0.002	0.003	0.001	0.000	0.001	0.001	0.056	0.040	0.043	0.028	0.037	0.095
OC	g/kg	0.044	0.086	0.020	0.011	0.012	0.024	0.143	0.121	0.106	0.056	0.113	0.165
SO_2	g/kg	2.22	1.40	1.84	1.64	1.89	2.51	1.99	1.06	1.80	1.13	1.95	2.06
NO_2	g/kg	0.091	0.091	0.069	0.046	0.075	0.080	0.019	0.039	0.004	0.001	0.002	0.008
NO	g/kg	8.27	6.25	6.34	3.75	5.58	11.9	5.05	2.49	4.51	3.48	4.57	5.96
TSP	g/kg	1.87	1.77	1.44	1.00	1.35	1.98	4.57	2.35	3.92	3.14	4.11	6.71
PM_{10}	g/kg	1.25	1.44	0.902	0.506	0.825	1.50	3.09	1.63	2.78	1.89	2.44	3.39
$PM_{2.5}$	g/kg	0.605	0.957	0.363	0.198	0.308	0.638	2.67	2.62	2.12	1.72	1.96	2.77
pPAHs(g)	mg/kg	0.608	0.459	0.394	0.260	0.472	0.919	1.88	1.82	1.48	1.15	1.48	1.96
pPAHs(p10)	mg/kg	0.217	0.255	0.122	0.051	0.110	0.268	0.915	0.73	0.685	0.43	0.561	1.43
pPAHs(p2.5)	mg/kg	0.080	0.090	0.045	0.019	0.051	0.116	0.516	0.36	0.409	0.223	0.426	0.722
nPAHs(g)	mg/kg	0.013	0.010	0.009	0.006	0.009	0.020	0.112	0.129	0.077	0.044	0.090	0.114
nPAHs(p10)	mg/kg	0.002	0.002	0.002	0.001	0.001	0.003	0.017	0.010	0.014	0.010	0.012	0.021
nPAHs(p2.5)	mg/kg	0.001	0.001	0.001	0.000	0.001	0.001	0.010	0.004	0.009	0.007	0.009	0.013
oPAHs(g)	mg/kg	0.129	0.123	0.068	0.040	0.078	0.204	0.953	1.17	0.642	0.329	0.646	1.047
oPAHs(p10)	mg/kg	0.031	0.032	0.021	0.011	0.019	0.039	0.134	0.097	0.107	0.066	0.086	0.184
oPAHs(p2.5)	mg/kg	0.007	0.006	0.004	0.002	0.006	0.009	0.078	0.051	0.064	0.041	0.061	0.118

Table 2
The EFs of various air pollutants measured for fugitive emissions from the two types of brick kilns. The statistics include the arithmetic means (M), standard deviations (SD), geometric means (GM), and the 25th, 50th, and 75th percentiles (p25, p50, and p75).

Pollutants	K-1						K-2						
	M	SD	GM	p25	p50	p75	M	SD	GM	p25	p50	p75	
CO_2	g/kg	578	11.9	578	570	582	587	403	92.7	394	366	372	409
CO	g/kg	26.9	7.67	25.9	21.2	24.9	31.9	123	48.7	111	97.6	141	165
EC	g/kg	0.04	0.03	0.03	0.02	0.03	0.07	0.16	0.21	0.05	0.01	0.03	0.26
OC	g/kg	0.63	0.36	0.55	0.43	0.51	0.81	1.66	1.88	0.82	0.24	1.32	2.18
SO_2	g/kg	2.34	1.03	2.11	1.91	2.22	2.70	2.60	3.74	0.98	0.23	1.00	2.02
NO_2	g/kg	0.01	0.01	0.01	0.00	0.01	0.01	0.02	0.01	0.01	0.01	0.01	0.03
NO	g/kg	0.72	0.85	0.58	0.33	0.58	0.80	1.33	1.46	0.86	0.48	0.62	1.12
TSP	g/kg	15.5	11.7	12.7	7.62	10.5	17.2	79.2	102	21.8	2.94	25.6	152
PM_{10}	g/kg	8.36	3.16	7.89	6.02	7.34	10.5	71.5	93.8	17.4	2.17	21.2	131
$PM_{2.5}$	g/kg	3.71	1.58	3.41	2.83	3.25	4.76	31.1	40.7	13.1	2.20	18.1	37.4
pPAHs(g)	mg/kg	6.22	5.67	3.78	2.60	3.11	9.45	3.01	3.21	1.61	1.18	1.81	3.28
pPAHs(p10)	mg/kg	19.4	21.0	12.7	7.08	8.31	24.7	33.7	43.6	12.5	4.30	17.2	32.8
pPAHs(p2.5)	mg/kg	3.33	4.16	1.99	1.23	1.62	3.23	9.23	10.98	5.00	3.02	4.39	12.1
nPAHs(g)	mg/kg	0.04	0.02	0.04	0.03	0.04	0.04	0.13	0.11	0.09	0.05	0.10	0.21
nPAHs(p10)	mg/kg	0.04	0.02	0.04	0.02	0.04	0.05	0.32	0.35	0.15	0.06	0.18	0.49
nPAHs(p2.5)	mg/kg	0.02	0.03	0.01	0.01	0.01	0.02	0.09	0.08	0.06	0.04	0.07	0.13
oPAHs(g)	mg/kg	0.39	0.36	0.26	0.18	0.26	0.41	1.30	0.98	0.78	0.60	1.17	2.13
oPAHs(p10)	mg/kg	1.65	1.71	1.14	0.59	0.86	1.85	2.75	3.37	1.28	0.47	1.75	3.39
oPAHs(p2.5)	mg/kg	0.25	0.28	0.15	0.10	0.13	0.35	0.78	0.64	0.50	0.30	0.69	1.16

in Fig. S4. Accordingly, the geometric means and standard deviations are listed as major descriptive statistics. The arithmetic means and standard deviations are also provided for an easier comparison because arithmetic, instead of geometric, statistics are often reported in the literature. Moreover, arithmetic statistics are required for total emission calculations (Huang et al., 2014; Wang et al., 2014). In addition, three quartiles, as non-parametric variables, are listed in the tables. The EFs for gaseous and particulate (bound to PM_{10} and $PM_{2.5}$) phase PAHs are reported separately. The detailed EF values of individual PAH compounds in both gaseous and particular phases are provided in Tables S3 and S4 for stack and fugitive emission sources, respectively.

To compare our results with those reported in the literature, only the EFs for stack flue gases are used since all data reported in the literature were measured at chimneys. The only EFs reported for brick kilns in China were those of TSP (89 ± 82 mg/m^3) and NOx (4.8 ± 0.80 g/kg) from two previous studies, which were on the same orders of magnitude as our measurements of 11 ± 8.8 mg/m^3 for TSP and 6.7 ± 4.4 g/kg for NOx (Zhao et al., 2013; National Bureau of Statistics of the People's Republic of China, 2009). Other field measurements have been conducted in India, and most brick kilns in India are Bull's type, which are different from those in China in terms of emissions (Maithel et al., 2012). According to the results of several studies conducted in India, the EFs measured for stack flue gases were considerably higher than our data, and the differences can be as high as orders of magnitude. For example, the EFs of $PM_{2.5}$, (8.4 ± 5.4 g/kg), BC (1.0 ± 1.2 g/kg), and OC (7.0 ± 4.3 g/kg) reported for fixed-chimney Bull's trench kilns burning domestic lignite in Calcutta, Chennai, Delhi, and Mumbai in India (Reddy and Venkataraman, 2002) were much higher than those found in this study (1.6 ± 2.0, 0.029 ± 0.022, and 0.094 ± 0.10 g/kg for $PM_{2.5}$, BC, and OC, respectively). A more recent study in India found that the EFs for similar Bull's brick kilns in Garh, Mukteshwar, Ludhiana, and Arah were 3.2 ± 0.70, 9.8 ± 4.8, 1.7 ± 1.3, and 0.30 ± 0.14 g/kg for $PM_{2.5}$, SO_2, EC, and OC (Maithel et al., 2012), respectively, which again were significantly higher than our measurements of 1.6 ± 2.0,

2.1 ± 1.2, 0.029 ± 0.022, and 0.094 ± 0.10 g/kg for the same pollutants. These differences are relatively large for incomplete combustion products, such as BC and OC, and small for pollutants from fuel composition, such as CO_2 and SO_2. This difference in the pollutant profile suggests that the different EFs between the brick kilns in China and those in India are primarily caused by the differences in kiln designs and, consequently, the combustion conditions rather than differences in fuel composition. However, the EFs of major air pollutants for the studied kilns are generally higher than those for tunnel kilns, which are widely used in developed countries and can be found occasionally in China (10%) and India (General Administration of Quality Supervision, 2013). For example, the EFs of TSP, PM_{10}, CO, and NOx for tunnel kilns in the United States were as low as 0.31 ± 0.045, 0.20 ± 0.042, 0.41 ± 0.022, and 0.32 ± 0.029 g/kg (U.S. EPA, 1997), respectively, which are much lower than those found in this study (3.2 ± 2.1, 2.2 ± 1.5, 330 ± 160, and 6.7 ± 4.4 g/kg for the same pollutants), likely due to the difference in combustion efficiency. In contrast, the EFs of fuel composition dependent SO_2 were similar between the annular kilns (2.1 ± 1.2 g/kg) in China and the tunnel kilns (0.95 ± 0.58 g/kg) in the United States. Presumably, similar types of coals were used.

3.2. EF differences between the stack and fugitive sources

Chimneys are designed to exhaust flue gas from the processes and are believed to be the major emission pathway of air pollutants. Therefore, EFs are often measured at chimneys and reported for stack flue gases in most studies. To the best of our knowledge, all of the studies on EFs for brick kilns, and likely for many other similar processes, were conducted in this manner (Baum, 2015; Maithel et al., 2012; Skinder et al., 2013). These EFs were then directly used to characterize the total emissions of air pollutants (Zhao et al., 2013; Reddy and Venkataraman, 2002; Zhang et al., 2009; Lei et al., 2011). However, similarly to many other facilities such as coke ovens and smelting furnaces, fugitive emission is unavoidable because the kiln furnace is not air sealed at all, and air pollutants can leak into the surrounding environment via non-chimney pathways. For the brick kilns studied, although there are two built-in air ducts connecting the entire furnace to the chimneys, the surface areas of the furnace roof with cracks and fuel feeding holes are as large as 400 (K-2) and 900 m^2 (K-1), through which considerable fugitive emission of various pollutants can occur. Moreover, there are no emission control facilities for such leakage. Indeed, smoke from the furnace roof can be observed with the naked eye (Fig. S5). Therefore, the overall emissions of air pollutants should be quantified based on both stack flue and fugitive sources; Otherwise, they would be underestimated. Unfortunately, this has never been performed before mainly due to technical difficulties in fugitive flow measurement.

Fig. 1 shows the two pathways of the emissions of major air pollutants from the brick kiln. With the measured emissions of various pollutants at both stack and fugitive sources, it was possible to apply the modified carbon balance method to characterize quantitatively the EFs for both pathways.

Therefore, it was possible to gather complete emission data. The separately measured EFs for stack and fugitive emissions are shown in Fig. 2, and the detailed data are seen in Table 1 and 2 The measured EFs of most air pollutants were remarkably different between the two. The EFs of SO_2 and all incomplete combustion products, including TSP, PM_{10}, $PM_{2.5}$, EC, OC, pPAHs, nPAHs, and oPAHs from the fugitive source, were significantly higher than those from the stack gas ($p < 0.05$). This was true for both kiln types, and the differences can be as high as one, sometime even two, orders of magnitude. For example, the EFs of $PM_{2.5}$ were 0.61 ± 1.0 and 2.7 ± 2.6 g/kg for the stack gas from the two kiln types and 3.7 ± 1.6 and 31 ± 41 g/kg for the fugitive gas. It appears that with very high EFs, the overall emissions would be underestimated substantially if fugitive emissions were ignored. The EF differences between the stack and fugitive sources can be explained by the fact that the pollutants generated during the process travel a short distance to the furnace ceiling and a long distance to the chimney. For example, for the K-1 kilns, the mean distance to the furnace ceiling is approximately 1.1 m, while the average distance to the chimney is approximately 14 m. The difference between the two distances (1.4 and 14 m) was similar for K-2 kilns. Since the temperature along the travel pathway is over 1000 °C, the quantities of the incomplete combustion products can be reduced significantly on the way to the chimney due to much longer reaction time.

In addition to the EF values, significant differences in the EF ratios of various pollutants were found between the stack and fugitive emissions, suggesting that the differences in EFs between the two pathways are pollutant dependent. For instance, PMs from the two sources were different in size distribution. The average ratios of EF($PM_{2.5}$)/EF (TSP) of the two kiln types were 0.32 ± 0.08 and 0.59 ± 0.13 for the stack gas and 0.24 ± 0.09 and 0.39 ± 0.15 for the fugitive gas, indicating that the PMs from the fugitive sources were coarser than those from the stacks ($p < 0.05$). This may be because coarse PMs were more readily removed during transport towards the chimneys than were the fine ones (Gillette, 1981). Because PAHs are more strongly associated with fine particles, the EF ratios of $PM_{2.5}$-bound PAHs (pPAHs, nPAHs, and oPAHs) to PM_{10}-bound PAHs (EF($PM_{2.5}$-PAHs)/EF(PM_{10}-PAHs)) for the stack gas flue were higher than those for the fugitive emissions ($p < 0.05$). For the same reason, the EF ratios of particulate and gaseous phase PAHs (EF(PAH(p))/EF(PAH(g))) were also lower in the stack flue than in the fugitive gas ($p < 0.05$). In contrast, the ratios of EF (EC)/EF(OC) were not significantly different ($p > 0.05$), indicating similar fates in the air duct.

3.3. Overall emission factors

Using the modified carbon balance method developed in this study, flow rates were derived from the fugitive emissions. Because of the large surface areas and numerous openings on the furnace roofs, the flow rates of the fugitive emission for the two kiln types were 16 ± 5.3 (K-1) and 7.6 ± 4.8 (K-2) m^3/s. In comparison, the flow rates measured directly at the stacks were 13.6 ± 3.5 and 5.9 ± 2.0 m^3/s. Therefore, the relative contributions of the fugitive leaks to the total exhaust flows were as high as 54 ± 11% and 56 ± 10%. With taller chimneys and higher power of the exhaust fans, the stack flows of K-1 kilns were much higher than those of the K-2 ones. The relatively high flow rates in air ducts can not only draw more pollutants to travel a longer distance within high-temperature furnaces but also create a relatively negative pressure to reduce fugitive emissions. Consequently, the overall emissions of the incomplete combustion products were substantially reduced.

Based on both the flow rates and the EFs measured for the stack and fugitive sources, the overall EFs of various air pollutants could be quantified by taking both stack and diffusive emissions into account. Because of the relatively high flow rates and EFs of most pollutants, the fugitive sources contributed the majority of the overall EFs. The overall emissions of many pollutants would be dramatically underestimated if only stack measurements were considered. The calculated overall EFs of various pollutants for the two kiln types are listed in Table S5. The relative contributions of the fugitive emissions to the overall EFs of variance pollutants were 73 ± 32% and 71 ± 28% for the two kiln types, demonstrating clearly the fugitive emission domination. The importance of fugitive emission from various industrial processes has been discussed, and

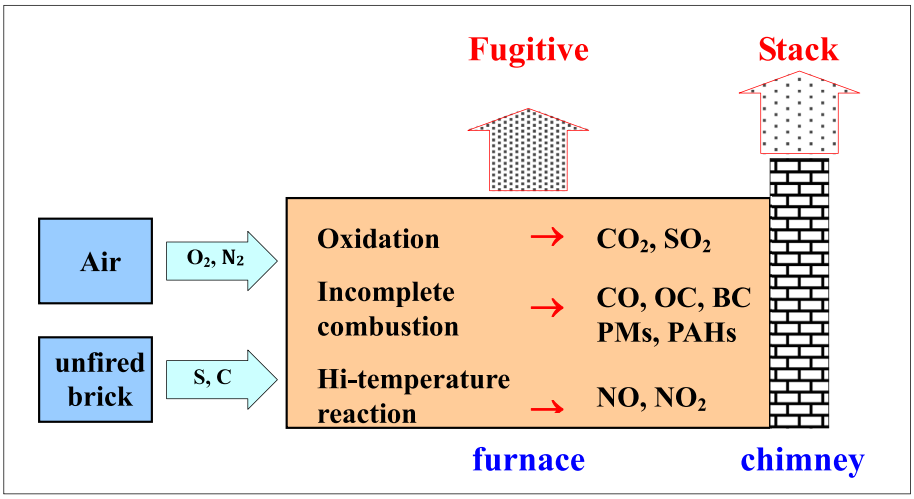

Fig. 1. Stack and fugitive emissions of major air pollutants from a typical brick kilns. The emissions of major air pollutants are from the oxidation of fuel components, incomplete combustion, or high-temperature reaction.

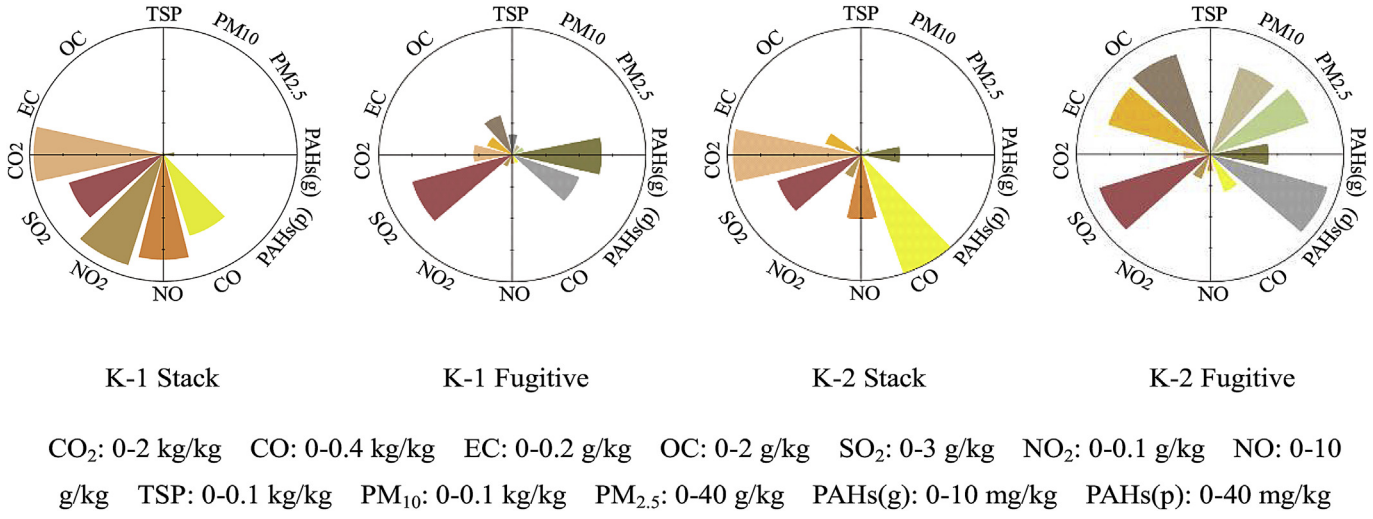

Fig. 2. The measured EFs of CO_2, CO, EC, OC, SO_2, NO_2, NO, TSP, PM_{10}, $PM_{2.5}$, pPAHs(g), and pPAHs(p) for brick kilns in China. Average EFs are shown for both stack (left panels) and fugitive (right panels) sources for the two types of kilns.

high concentrations of various pollutants in fugitive emissions have been reported occasionally (Kurokawa et al., 2013; Pham et al., 2008; Eklund, 1992). However, the quantification of fugitive emissions has always been a challenge mainly due to the difficulty in fugitive flow rate measurement. In this study, the modified carbon balance method was effective in solving this problem.

Relatively high uncertainty in the reported data could not be avoided for the following reasons: 1) the fugitive emissions were measured using limited samples collected on a large furnace roof; 2) the flow rates of the fugitive emission could not be measured directly, and errors can be introduced by the calculation; 3) other fugitive sources in addition to the furnace roofs, such as side walls, were not examined; and 4) the number of kilns sampled was small, and high variations are expected among them; however, it would be too costly and time consuming to sample more kilns, which are everywhere in China. Still, with the fugitive emissions taken into consideration, the new method developed in this study is a great improvement over the previous approach.

Although a similar set of pollutants are emitted from various residential and industrial sources, including brick kilns, the EFs of different air pollutants for combustion sources are governed by many factors. For example, SO_2 emission is fuel composition dependent, and EFs of SO_2 were similar between brick kilns (4.6 g/kg) and other industrial processes, such as coal-fired power stations (7.8 g/kg), since similar coals were used (Zhang et al., 2009; Chen et al., 2016d). The EFs of NOx, as a high-temperature reaction product (Aho et al., 1995), were similar among brick kilns (7.8 g/kg), coal-fired power plants (7.8 g/kg), and cement kilns (6.0 g/kg) because of similar combustion temperatures (Zhang et al., 2009; Vaillant et al., 2008). In contrast, large variations were found in incomplete combustion products, such as CO, PM, BC, and PAHs. The EFs of these pollutants for brick kilns measured in this study were similar to those for residential stoves but were orders of magnitude higher than those for coal-fired power stations, iron/steel plants, or cement kilns. For example, the EFs of CO were 410 ± 190 g/kg for brick kilns and 59 and 121 g/kg for iron/steel and cement production (Zhang et al., 2009). The EF of $PM_{2.5}$ for brick production was 19 ± 23 g/kg, which was close to that of residential stoves (9.6 g/kg) but much higher than 2.0 and 0.85 for coal-fired power stations and iron/steel production (Zhang et al., 2009;

Chen et al., 2016d). The EFs of BC were similar between brick kilns and residential sources (Chen et al., 2016d; Streets et al., 2001). In comparison, the EFs of BC for coal-fired power stations could be as low as 0.0035 g/kg due to much better combustion conditions (Wang et al., 2014). A similar trend was also found in parent PAHs among brick kilns (33 ± 38 mg/kg), residential stoves (200 mg/kg) (Shen et al., 2013b), and coal-fired power stations (0.6 mg/kg) (Yang et al., 1998).

3.4. Differences between the two kiln types

For the two types of kilns, the designs and operations were different. It is expected, therefore, that the EFs of various pollutants would also be different. To confirm the difference quantitatively, a set of two-way nested ANOVAs were conducted for the overall EFs of each pollutant for the individual kilns nested within the kiln types in the model. The calculated *p*-values of the two factors (kiln types and individual kilns) in log-scale are shown as a bar chart in Table S6.

For the majority of incomplete combustion products, including TSP, PM_{10}, $PM_{2.5}$, EC, OC, and all PAHs, the EF differences between the two kiln types were more significant than the differences among the individual kilns, indicating a remarkable difference in combustion efficiencies between the two kiln types. According to the results of the model-II supplemental analysis following the ANOVA, the components of variance for the kiln type contribute 48–83% of the overall EF variance, which is much higher than for the individual kilns (16–40%). For most incomplete pollutants, the EFs for the K-2 kilns were higher than those for the K-1 kilns, and most differences were statistically significant ($p < 0.05$). The differences were as high as 4.8–7.8 times for PMs, 2.7–4.8 times for EC and OC, 1.7–7.6 times for PAHs (all), and 1.5–2.1 times for CO. It appears that the oxygen supply of the K-2 kilns was poorer than that of the K-1 kilns. As mentioned in the Methods section, the chimneys of the K-1 kilns were made of bricks 20–30 m in height and 2–3 m in diameter, while the iron chimneys of the K-2 kilns were merely 1 m in height. Thus, the average stack flow rate of the K-1 kilns (14 ± 3.5 m^3/s) was much higher than that of the K-2 kilns (5.9 ± 2.0 m^3/s) ($p < 0.05$). Furthermore, the higher density of the loaded bricks in the K-1 kilns (370 bricks/m^3) and smaller kiln furnace (height: 2–2.5 m; length: 30 m; width: 8 m) led to a relatively poorer air supply compared with the K-2 kilns (300 bricks/m^3, 4.5 m in height, 60 m in length, and 15 m in width).

Unlike the EFs of the incomplete combustion products, the differences in the overall EFs of CO_2 and SO_2 between the two kiln types were not significant ($p > 0.05$) because they are dependent on fuel composition rather than on combustion condition. The EF differences of NO and NO_2 between the two types of the kilns were opposite as they are incomplete combustion products. Although the differences were not statistically significant due to high variations ($p > 0.05$), the EFs of NO and NO_2 for the K-1 kilns (9.0 ± 7.1 and 0.10 ± 0.10 g/kg) were higher than those of the K-2 kilns (6.4 ± 5.4 and 0.039 ± 0.049 g/kg), which can be reasonably explained by the relatively higher temperatures in the K-1 kilns (1372 ± 322 °C) compared with those in the K-2 kilns (1125 ± 266 °C).

It is also interesting but not surprising to note that not only were the absolute EF values different between the kiln types and among the individual kilns, but the EF ratios of some closely related pollutants, such as EF($PM_{2.5}$)/EF(PM_{10}), EF (EC)/EF(OC), and EF(PAH(p))/EF(PAH(g)), were different to a certain extent. In some cases, these ratios are also important in terms of influences on environmental quality, climate, and human health. For instance, fine PMs have a stronger influence on visibility (Seinfeld and Pandis, 2016) and can penetrate deeper in the respiratory tract, causing more damage to health (Valavanidis et al., 2008). Gaseous phase PAHs can be removed faster than particulate phase ones, resulting in lower long-range transport potential (Shen et al., 2013b; Rianawati, 2007). According to our results, the K-2 kilns emitted not only more PMs but also more fine particles, leading to a significantly ($p < 0.05$) higher ratio of EF($PM_{2.5}$)/EF(PM_{10}) for the K-2 (0.48 ± 0.15) than the K-1 (0.35 ± 0.13) kilns. The relatively higher emissions and fine particle fractions from the K-2 kilns can be explained by the relatively poor combustion conditions. The mean contribution efficiencies of the K-1 and K-2 kilns were 90 ± 9% and 82 ± 5%, respectively. It has been well demonstrated that more emissions, especially emissions of fine particles, can result from lower combustion efficiency (Shen et al., 2012). Similarly, the EF(PAH(p))/EF(PAH(g)) ratio for the K-2 kilns was significantly higher than that for the K-1 kilns ($p < 0.05$). In contrast, EF (EC)/EF(OC) for the K-2 kilns (0.12 ± 0.05) was much higher than that of the K-1 kilns (0.062 ± 0.026) ($p < 0.05$), which agrees with the fact that intensive burning processes can cause higher EC/OC ratios due to worse air-fuel mixing status (Shen et al., 2014; Roden et al., 2009).

The EFs of various pollutants for the two kiln types were compared for both stack and fugitive emissions by plotting the EFs of the K-1 kilns against those of the K-2 kilns in Fig. S6. The EFs of the incomplete combustion products from the stack sources were orders of magnitude lower than those from the fugitive sources in log-scale. The differences in the EFs between the two kiln types can also be observed as the majority of the data points fall below the 1:1 line except for NOx, CO_2, and SO_2.

3.5. Relationship among various pollutants

A variety of air pollutants is emitted from brick kilns simultaneously. The relationship among the pollutants is associated with the mechanisms of the pollutant generation. Therefore, the emissions of various pollutants are dependent on either the fuel properties and/or the combustion conditions. The relationship among all pollutants studied is shown in a correlation matrix for overall EFs including both stack and fugitive sources (Table S7). Fig. 3 shows the correlations between a few typical pollutants. In general, there were positive correlations among the EFs of all incomplete combustion products, including PMs (TSP, PM_{10}, and $PM_{2.5}$), organic and elemental carbons (OC and EC), PAHs (pPAHs, nPAHs, and oPAHs), and CO. Meanwhile, the EFs of NO and NO_2 were often negatively correlated with the EFs of incomplete combustion products because the EFs of both NOx and incomplete combustion products are associated with combustion conditions, including temperature, oxygen supply, and combustion efficiency (Chen et al., 2016a; Koppejan, 2012; Gurney et al., 2009; United Research Services, 2003), but in opposite directions. In contrast, the EFs of SO_2 and CO_2 were independent of the EFs of other pollutants, which can be explained by the fact that emissions of SO_2 and CO_2 are fuel composition (sulfur and carbon) dependent.

This relationship among all pollutants can also be summarized in a vector cosine angle based dendrogram, as shown in Fig. S7. The PAHs are clustered at one end with close association with PMs, including BC and OC. These are all incomplete combustion products, and their emissions were higher when the combustion efficiency was lower (Chen et al., 2016a; Shen et al., 2011). The other pollutants are either high-temperature products, such as NOx (Aho et al., 1995), or released fuel components (SO_2 and CO_2), which appear at another end of the dendrogram. If the cluster analysis was conducted for the two kiln types separately or using Euclidean distance instead of vector cosine angle (Fig. S8), the results would be more or less similar to that shown in Fig. S7, indicating that the two categories of pollutants are distinguished robustly not only in relative but also in absolute terms.

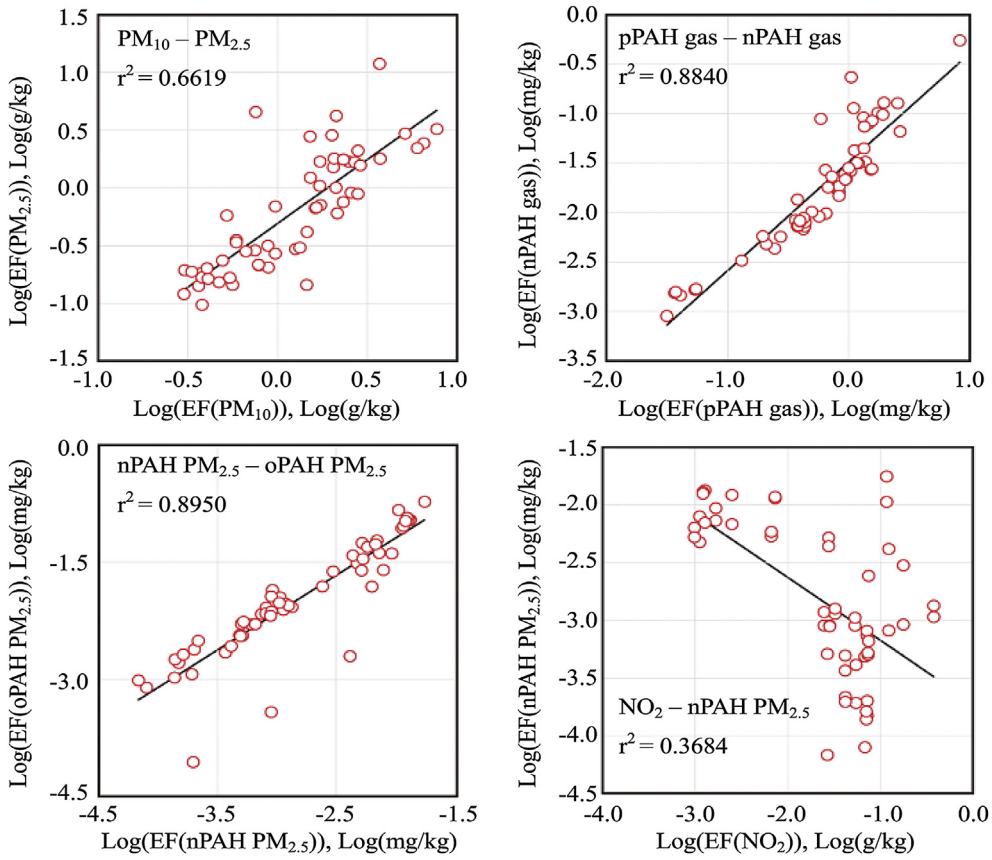

Fig. 3. Correlations between the EFs of $PM_{2.5}$ and PM_{10}, the EFs of gaseous phase pPAHs and nPAHs, the EFs of $PM_{2.5}$ bound nPAHs and oPAHs, and the EFs of NO_2 and $PM_{2.5}$ bound nPAHs.

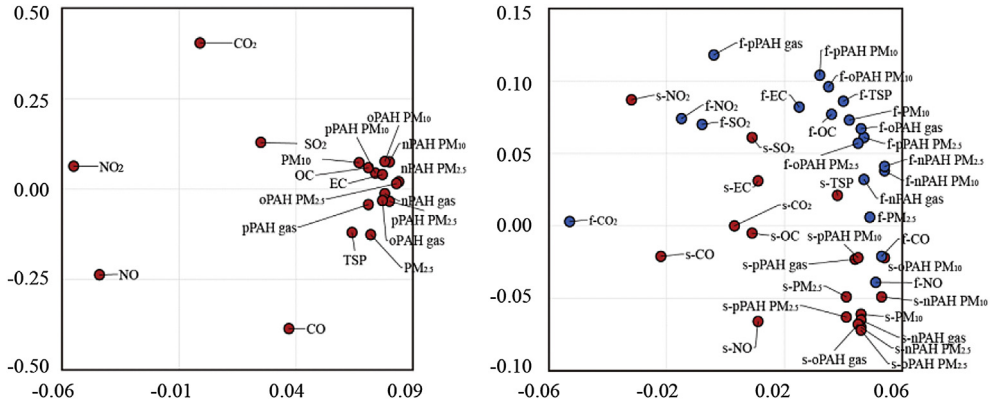

Fig. 4. Factor score plot of F1 against F2 derived from the principal component analysis. The analyses were conducted with stack and fugitive emissions combined (left panel) or individually (right panel). The **red** and **blue** data points in right panel represent either stack or fugitive emissions. (For interpretation of the references to colour in this figure legend, the reader is referred to the web version of this article.)

This distinction can be further illustrated by a principal component analysis. The result is presented in Fig. 4 (left panel) as a factor score plot of the first component (F1) against the second (F2). More than 60% of the variance can be explained by the first component, which distinguishes the incomplete combustion products from the others. Those having relatively high F1 values, including PMs, OC, EC, and PAHs, are associated with relatively low combustion efficiency, while NOx, as a high-temperature reaction product, appears at the low F1 end. Approximately 14% of the overall variance can be explained by the second component. Although the F2 of most incomplete combustion products are similar to one another, CO_2, CO, NO_2 and NO are well distinguished along the F2 axis. It was previously reported that the ratios of NO/NO_2 and CO/CO_2 depend on the combustion temperature (Aho et al., 1995; Sulzmann et al., 1965; Jin et al., 1987). When the EFs of various pollutants from the stack and fugitive emissions are used separately in a principal component analysis, the plot of F1 against F2 (Fig. 4, right panel) can provide further information regarding the differences between the two sources. Similar to the results for the overall EFs, F1 represents the completeness of the combustion

(46% of the total variance), and the incomplete combustion products from both stack and fugitive sources appear at the right side of the plot. Meanwhile, they are well separated along the vertical direction of F2 with only a few exceptions. Compared with the analysis with two sources combined, the contribution of F2 to the total variance increased to 23%. As discussed above, the F2 mainly represents the combustion temperature. This time, not only were CO, CO_2, NO, and NO_2 separated by F2, but the EFs of the incomplete combustion products were also distinguished, with generally positive F2 score values of fugitive emission EFs and negative F2 scores of stack emission EFs.

4. Conclusions

For the major pollutants, the EFs for the China's brick kilns (annular kilns) were much higher than those for the relatively advanced brick kilns - tunnel kilns in developed countries, and significantly lower than those for Bull's type brick kilns in India. Based on the new modified carbon balance method, it was found that EFs for the major pollutants of fugitive emissions from brick roofs were much higher than those measured at the stacks. Overall EFs for the brick kilns were calculated by combining the fugitive emission with stack emission, resulting higher emission compared with neglecting the fugitive source. The new method for estimating fugitive emission could be utilized in the further study for similar combustion devices.

Conflict of interest

The authors declare no competing financial interest from this paper.

Acknowledgements

This work was supported by the National Natural Science Foundation of China (41390240 and 41571130010) and the 111 Project (B14001).

Appendix A. Supplementary data

Supplementary data related to this chapter can be found at http://dx.doi.org/10.1016/j.envpol.2017.02.022.

References

Adgate, J.L., Ramachandran, G., Pratt, G.C., Waller, L.A., Sexton, K., 2002. Spatial and temporal variability in outdoor, indoor, and personal $PM_{2.5}$ exposure. Atmos. Environ. 36 (20), 3255–3265.

Aho, M.J., Paakkinen, K.M., Pirkonen, P.M., Kilpinen, P., Hupa, M., 1995. The effects of pressure, oxygen partial pressure, and temperature on the formation of N_2O, NO, and NO_2 from pulverized coal. Combust. Flame 102 (3), 387–400.

Baum, E., 2015. Emissions from S Asian Brick Production & Potential Climate Impact. Climate & Health Research Network at the Anil Agarwal Dialogue 2015. Poor in Climate Change. India Habitat Centre, New Delhi, India.

Centre for Science and Environment, 2015. Overview on Brick Kiln: Pollution, Technology and where We Need to Go? Centre for Science and Environment, New Delhi, India. http://www.cseindia.org/docs/aad2015/Overview2.pdf.

Chen, Y., Shen, G., Su, S., Du, W., Huangfu, Y., Liu, G., Wang, X., Xing, B., Smith, K.R., Tao, S., 2016a. Efficiencies and pollutant emissions from forced-draft biomass-pellet semi-gasifier stoves: comparison of International and Chinese water boiling test protocols. Energy sustain. Dev. 32, 22–30.

Chen, Y., Shen, G., Huang, Y., Zhang, Y., Han, Y., Wang, R., Shen, H., Su, S., Lin, N., Zhu, D., Pei, L., Zheng, X., Wu, J., Wang, X., Liu, W., Wong, M., Tao, S., 2016b. Household air pollution and personal exposure risk of polycyclic aromatic hydrocarbons among rural residents in Shanxi, China. Indoor Air 26 (2), 246–258.

Chen, Y., Du, W., Shen, G., Zhuo, S., Zhu, X., Shen, H., Huang, Y., Su, S., Lin, N., Pei, L., Zheng, X., Wu, J., Duan, Y., Wang, X., Liu, W., Wong, M., Tao, S., 2016c. Household air pollution and personal exposure to nitrated and oxygenated polycyclic aromatics (PAHs) in rural households: influence of household cooking energies. Indoor Air 27 (1), 169–178.

Chen, Y., Shen, G., Liu, W., Du, W., Su, S., Duan, Y., Lin, N., Zhuo, S., Wang, X., Xing, B., Tao, S., 2016d. Field measurement and estimate of gaseous and particle pollutant emissions from cooking and space heating processes in rural households, northern China. Atmos. Environ. 125, 265–271.

Eklund, B., 1992. Practical guidance for flux chamber measurements of fugitive volatile organic emission rates. J. Air Waste Manage 42 (12), 1583–1591.

General Administration of Quality Supervision, 2013. Emission Standard of Air Pollutants for Brick and Tile Industry in Inspection and Quarantine of P.R.C. Ministry of Health of P.R.C Bureau of Environmental Protection of P.R.C, Beijing, China, pp. 29620–32013. GB.

Gillette, D.A., 1981. Production of dust that may be carried great distances. Geo. Soci. Amer. Spec. Pap. 11–26.

Gurney, K.R., Mendoza, D.L., Zhou, Y., Fischer, M.L., Miller, C.C., Geethakumar, S., Can, S.D.L.R.D., 2009. High resolution fossil fuel combustion CO_2 emission fluxes for the United States. Environ. Sci. Technol. 43 (14), 5535–5541.

Guttikunda, S., 2015. Particulate Pollution and its Health Impacts from Brick Kiln Clusters in South Asian Cities. Climate & Health Research Network at the Anil Agarwal Dialogue 2015. Centre for Science and Environment, India Habitat Centre, New Delhi, India.

Huang, Y., Shen, H., Chen, H., Wang, R., Zhang, Y., Su, S., Chen, Y., Lin, N., Zhuo, S., Zhong, Q., 2014. Quantification of global primary emissions of $PM_{2.5}$, PM_{10}, and TSP from combustion and industrial process sources. Environ. Sci. Technol. 48 (23), 13834–13843.

Jin, T., Okuhara, T., Mains, G.J., White, J.M., 1987. Temperature-programmed desorption of CO and CO_2 from Pt/CeO_2. An important role for lattice oxygen in CO oxidation. J. Phys. Chem. 91 (12), 3310–3315 (12).

Kan, H., Chen, R., Tong, S., 2012. Ambient air pollution, climate change, and population health in China. Environ. Int. 42 (1), 10–19.

Koppejan, J., 2012. The Handbook of Biomass Combustion and Co-firing. Routledge, London, UK. Reprint edition.

Kurokawa, J., Ohara, T., Morikawa, T., Hanayama, S., 2013. Emissions of air pollutants and greenhouse gases over Asian regions during 2000–2008: regional emission inventory in Asia (REAS) version 2. Atmos. Chem. Phys. 13 (4), 10049–10123.

Lei, Y., Zhang, Q., He, K.B., Streets, D.G., 2011. Primary anthropogenic aerosol emission trends for China, 1990–2005. Atmos. Chem. Phys. Discuss. 11 (3), 931–954.

Maithel, M., Lalchandani, D., Malhotra, G., Bhanware, P., Uma, R., Ragavan, S., Athalye, V., KR, B., Reddy, S., Bond, T., Weyant, C., Baum, E., Thoa, V., Phuong, T., Thanh, K., 2012. Brick kilns Performance Assessment. A Roadmap for Cleaner Brick Production in India: Executive Summary. Clean Air Task Force, New Delhi, India. http://www.ccacoalition.org/sites/default/files/resources/Brick_Kilns_Performance_Assessment.pdf.

Matus, K., Nam, K.M., Selin, N.E., Lamsal, L.N., Reilly, J.M., Paltsev, S., 2011. Health damages from air pollution in China. Global Environ. Change 22 (1), 55–66.

National Bureau of Statistics of the People's Republic of China, 2013. China statistical Yearbook. Beijing, China.

National Bureau of Statistics of the People's Republic of China, 2009. Description on Developing the Emission Standard of Pollutants for Brick and Tile Industry (Draft). Beijing, China.

Peng, C., Chen, W., Liao, X., Wang, M., Ouyang, Z., Jiao, W., Bai, Y., 2011. Polycyclic aromatic hydrocarbons in urban soils of Beijing: status, sources, distribution and potential risk. Environ. Pollut. 159 (3), 802–808.

Pham, T.B.T., Manomaiphiboon, K., Vongmahadlek, C., 2008. Development of an inventory and temporal allocation profiles of emissions from power plants and industrial facilities in Thailand. Sci. Total Environ. 397 (1–3), 103–118.

Reddy, M.S., Venkataraman, C., 2002. Inventory of aerosol and sulphur dioxide emissions from India: I—fossil fuel combustion. Atmos. Environ. 36 (4), 677–697.

Rianawati, E., 2007. Occurrence and Distribution of PAHs in Rainwater and Urban Runoff. National University of Singapore. Thesis for the Degree of Master of Engineering, Singapore.

Roden, C.A., Conway, B.S., Pinel, A.B.O., Maccarty, N., Still, D., 2009. Laboratory and field investigations of particulate and carbon monoxide emissions from traditional and improved cookstoves. Atmos. Environ. 43 (6), 1170–1181.

Seinfeld, J., Pandis, S., 2016. Atmospheric Chemistry and Physics: from Air Pollution to Climate Change. John Wiley & Sons, New York, USA.

Shen, H., Huang, Y., Wang, R., Zhu, D., Li, W., Shen, G., Wang, B., Zhang, Y., Chen, Y., Lu, Y., 2013a. Global atmospheric emissions of polycyclic aromatic hydrocarbons from 1960 to 2008 and future predictions. Environ. Sci. Technol. 47 (12), 6415–6424.

Shen, G., Yang, Y., Wang, W., Tao, S., Zhu, C., Min, Y., Xue, M., Ding, J., Wang, B., Wang, R., 2010. Emission factors of particulate matter and elemental carbon for crop residues and coals burned in typical household stoves in China. Environ. Sci. Technol. 44 (18), 7157–7162.

Shen, G., Wang, W., Yang, Y., Ding, J., Xue, M., Min, Y., Zhu, C., Shen, H., Li, W., Wang, B., Wang, R., Wang, X., Tao, S., Russell, A.G., 2011. Emissions of PAHs from indoor crop residue burning in a typical rural stove: emission factors, size distributions, and gas-particle partitioning. Environ. Sci. Technol. 45 (4), 1206–1212.

Shen, G., Tao, S., Chen, Y., Zhang, Y., Wei, S., Xue, M., Wang, B., Wang, R., Lu, Y., Li, W., Shen, H., Huang, Y., Chen, H., 2013b. Emission characteristics for polycyclic aromatic hydrocarbons from solid fuels burned in domestic stoves in rural China. Environ. Sci. Technol. 47 (24), 14485–14494.

Shen, G., Tao, S., Wei, S., Zhang, Y., Wang, R., Wang, B., Li, W., Shen, H., Huang, Y., Chen, Y., 2012. Reductions in emissions of carbonaceous particulate matter and polycyclic aromatic hydrocarbons from combustion of biomass pellets in

comparison with raw fuel burning. Environ. Sci. Technol. 46 (11), 6409–64016.
Shen, G., Xue, M., Chen, Y., Yang, C., Li, W., Shen, H., Huang, Y., Zhang, Y., Chen, H., Zhu, Y., 2014. Comparison of carbonaceous particulate matter emission factors among different solid fuels burned in residential stoves. Atmos. Environ. 89 (2), 337–345.
Skinder, B.M., Sheikh, A.Q., Pandit, A.K., Ganai, B.A., 2013. Brick kiln emissions and its environmental impact: a Review. J. Ecol. Nat. Environ. 6 (1), 1–11.
Smith, K.R., 1987. Biofuels, Air Pollution, and Health: a Global Review. Springer Science & Business Media, New York, USA.
Streets, D.G., Gupta, S., Waldhoff, S.T., Wang, M.Q., Bond, T.C., Bo, Y., 2001. Black carbon emissions in China. Atmos. Environ. 35 (25), 4281–4296.
Sulzmann, K.G.P., Myers, B.F., Bartle, E.R., 1965. CO oxidation. I. induction period preceding CO_2 formation in shock - heated CO-O_2-Ar mixtures. J. Chem. Phys. 42 (11), 3969–3979.
United Research Services, 2003. Greenhouse Gas Emission Factor Review, Final Technical Memorandum. United Research Services Corporation, Austin, TX, USA. http://s3.amazonaws.com/zanran_storage/www.edison.com/ContentPages/933104122.pdf.
U. S. Environmental Protection Agency, 1997. Brick and Structural Clay Product Manufacturing. NC, USA. https://www3.epa.gov/ttnchie1/ap42/ch11/final/c11s03.pdf.
Vaillant, J.C., Vandenberghe, B., Hahn, B., Heuser, H., Jochum, C., 2008. T/P23, 24, 911 and 92: new grades for advanced coal-fired power plants - properties and experience. Int. J. Pres. Ves. Pip. 85, 38–46.
Valavanidis, A., Flotakis, K., Vlachogianni, T., 2008. Airborne particulate matter and human health: toxicological assessment and importance of size and composition of particles for oxidative damage and carcinogenic mechanisms. J. Environ. Sci. Heal. C 26 (4), 339–362.
Wang, R., Tao, S., Shen, H., Huang, Y., Chen, H., Balkanski, Y., Boucher, O., Ciais, P., Shen, G., Li, W., 2014. Trend in global black carbon emissions from 1960 to 2007. Environ. Sci. Technol. 48 (12), 6780–6787.
Yang, H.H., Lee, W.J., Chen, S.J., Lai, S.O., 1998. PAH emission from various industrial stacks. J. Hazard. Mater 60 (2), 159–174.
Zhang, Z., 1997. Energy efficiency and environmental pollution of brickmaking in China. Energy 22 (1), 33–42.
Zhang, Q., Streets, D.G., Carmichael, G.R., He, K.B., Huo, H., Kannari, A., Klimont, Z., Park, I.S., Reddy, S., Fu, J.S., 2009. Asian emissions in 2006 for the NASA INTEX-B mission. Atmos. Chem. Phys. Discuss. 9 (14), 5131–5153.
Zhao, B., Wang, S.X., Liu, H., Xu, J.Y., Fu, K., Klimont, Z., Hao, J.M., He, K.B., Cofala, J., Amann, M., 2013. NOx emissions in China: historical trends and future perspectives. Atmos. Chem. Phys. 13 (6), 16047–16112.